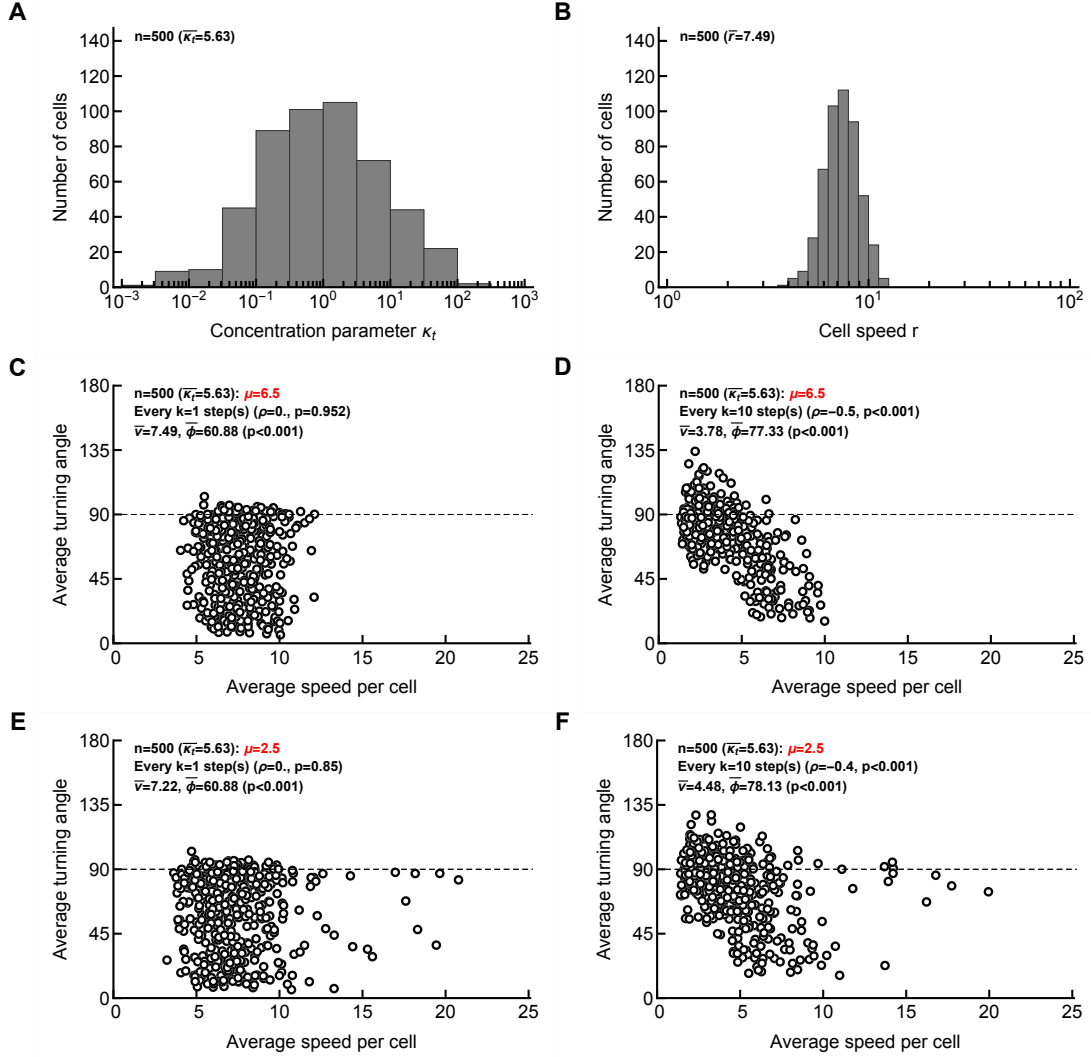


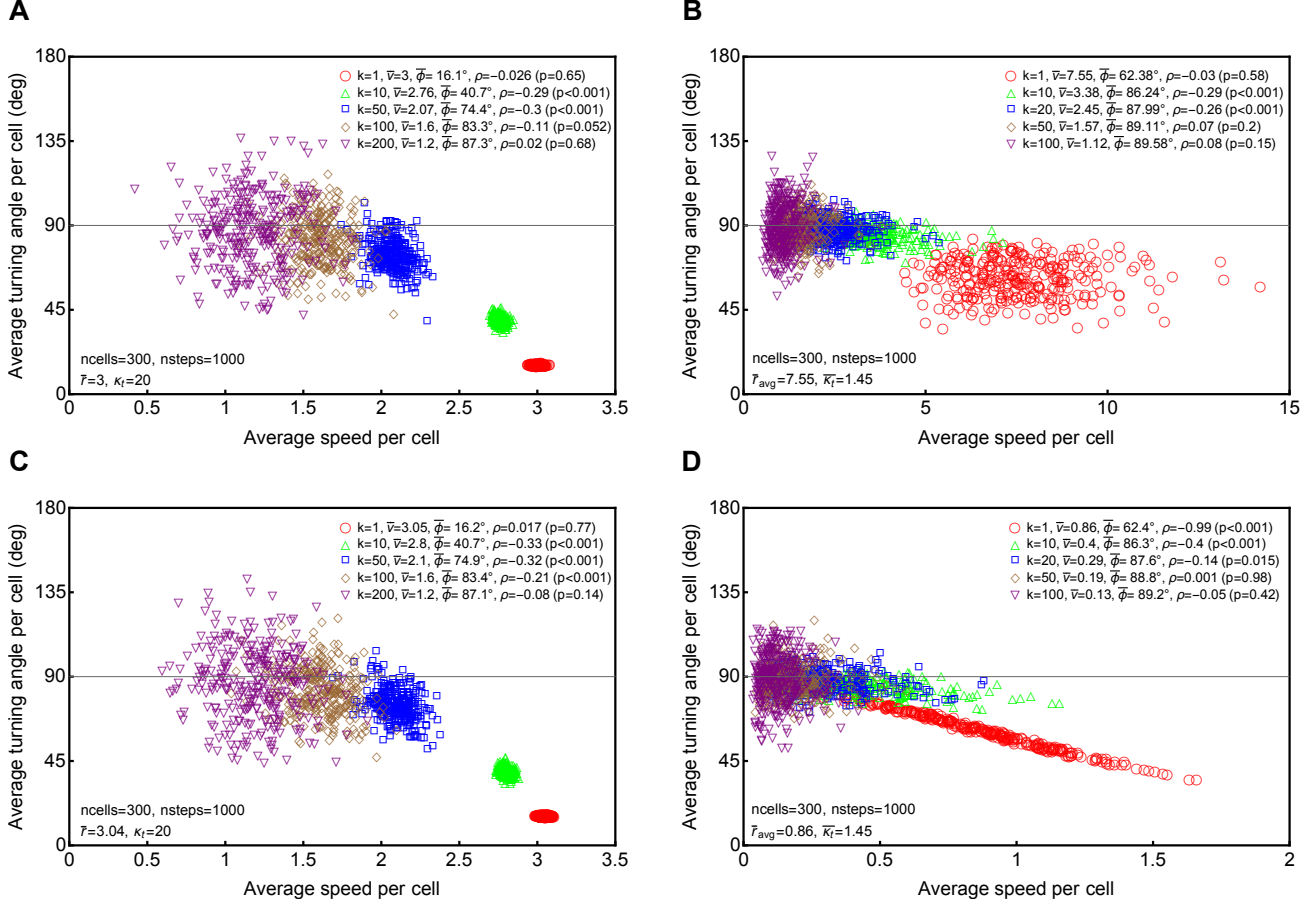
Correlation between speed and turning naturally arises for
sparsely sampled cell movements

Vitaly V. Ganusov, Viktor S. Zenkov, and Barun Majumder

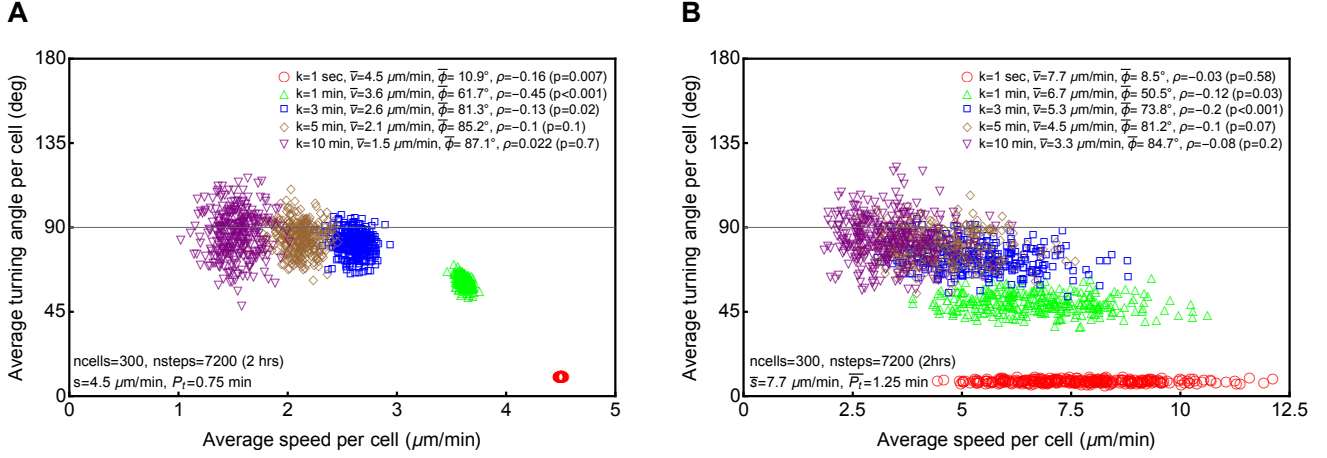
Supplemental Information



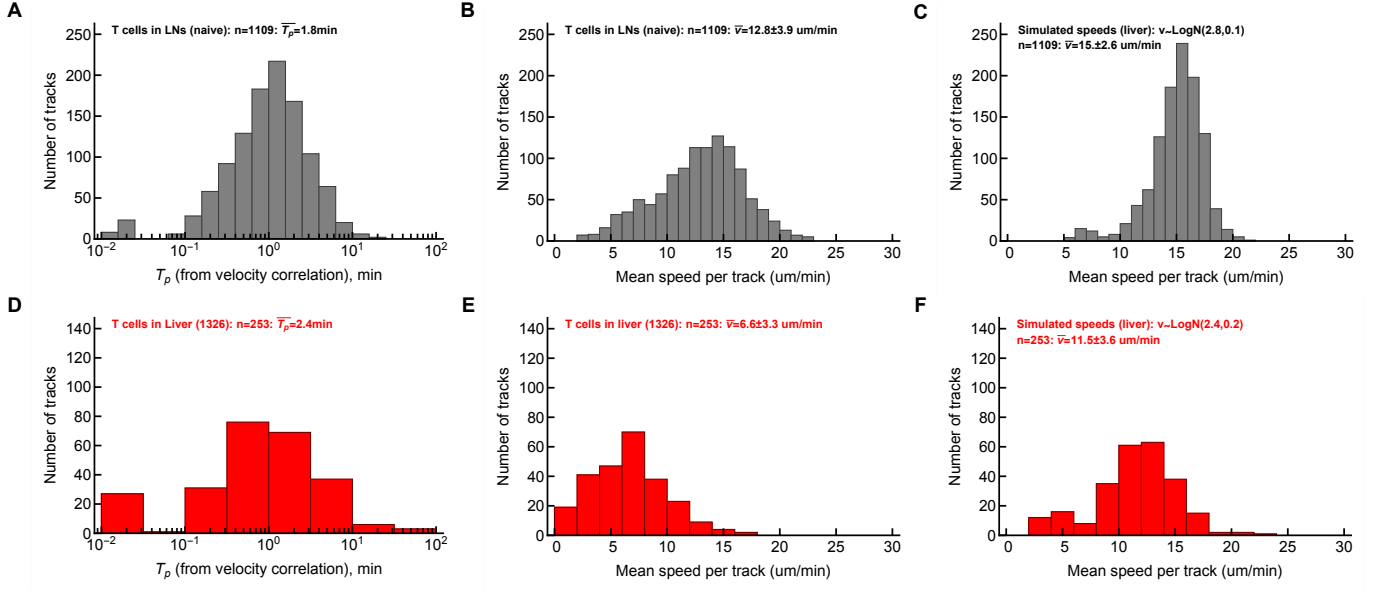
Supplemental Figure S1: Negative correlation between turning and speed arises when cells undergo Brownian walks or Levy flights. We simulated movement of cells using vMF distribution with both concentration parameter κ_t and movement lengths distributed log-normally (panels A-B, eqn. (4)) assuming that shape parameter of the Pareto distribution (eqn. (3)) is $\mu = 1 + \alpha = 6.5$ (panels C-D) or $\mu = 2.5$ (panels E-F) corresponding to Brownian walks ($\mu > 3$) or Levy walks/flights ($\mu < 3$). Cell trajectories were sampled either for every $k = 1$ movement (panels C&E) or every $k = 10^{\text{th}}$ movement (panels D&F). Other parameters are the same as in **Figure 2G-F**. We also plot the average concentration parameter $\bar{\kappa}_t$, average speed \bar{v} , and average turning angle $\bar{\phi}$. Spearman rank correlation coefficient ρ and associated p-values are indicated on individual panels (C-F). To fix the average movement lengths the same for simulations with $\mu = 2.5$ and $\mu = 6.5$, we changed r_{\min} for different μ as $r_{\min} = \bar{r}\mu/(\mu + 1)$ where \bar{r} is the average movement length for a given cell (chosen from panel B).



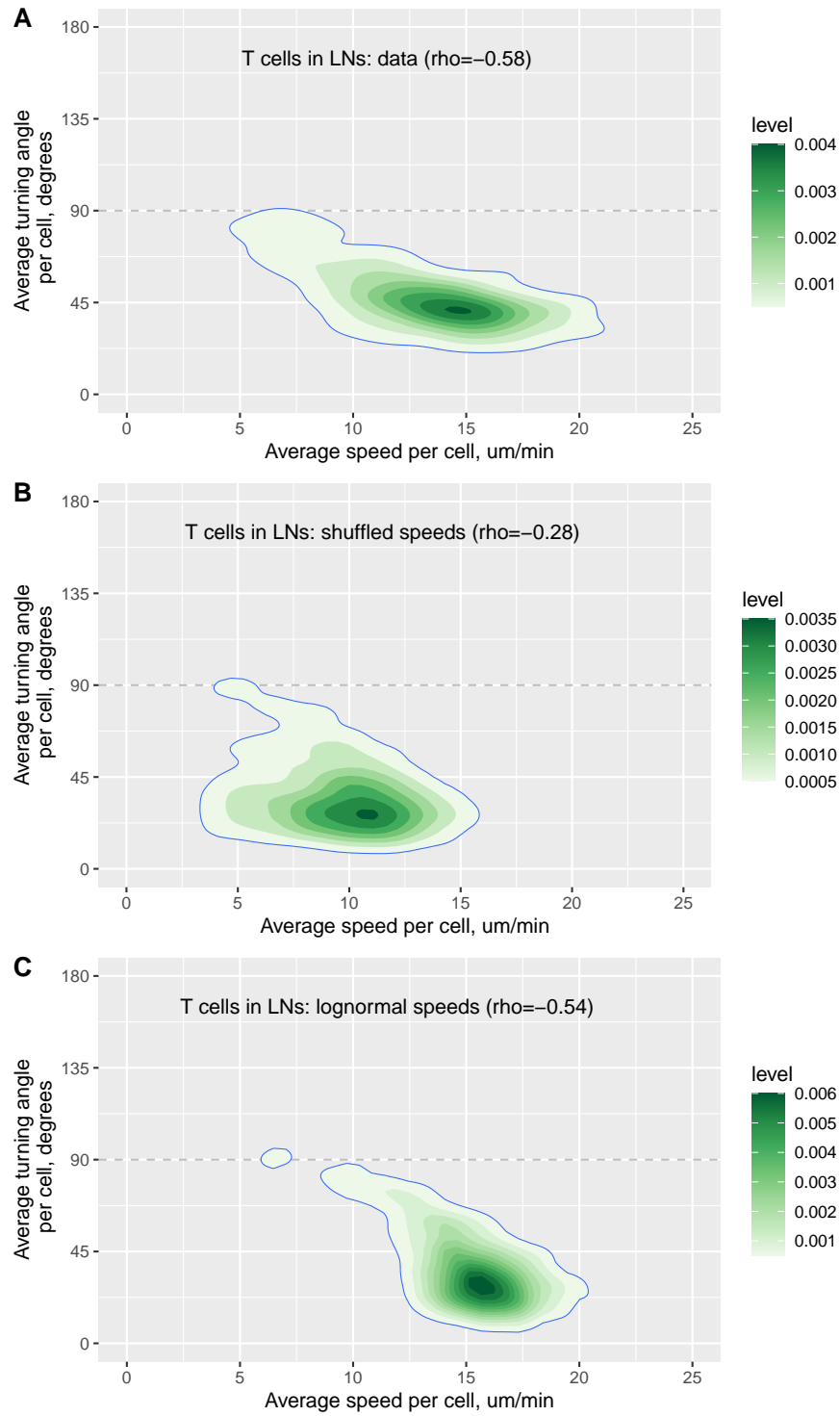
Supplemental Figure S2: Correlation between speed and turning angle disappears for coarsely sub-sampled simulation data generated using vMF distribution. We simulated 300 cells each with 10^3 steps using vMF distribution and sampled every k^{th} movements (k is indicated on individual panels). In panels A-B we assume that speed and concentration parameter κ_t are uncorrelated, and in panels C-D, speed is determined by κ_t via $\bar{r} = \ln(1 + \kappa_t)$. In panels A and C we assume that every cell have the same persistence defined by $\kappa_t = 20$ and same speed defined by $\bar{r} = 3$. In panels B and D we assume that every cell in the population has a different κ_t which was drawn from a lognormal distribution (eqn. (4) with $\mu = 0.2$ and $\sigma = 0.5$). In panel B, every cell has a random speed determined by \bar{r} in the Pareto distribution (\bar{r} was drawn from a lognormal distribution with $\mu = 2$ and $\sigma = 0.2$), and in panel D speeds are directly determined by κ_t as $\bar{r} = \ln(1 + \kappa_t)$. Average speed \bar{v} and average turning angle $\bar{\phi}$ for all cells are indicated on the panels, and statistical significance of the correlation between speed and turning angle per cell was determined using Spearman rank test (with the correlation coefficient ρ and p-values are shown on individual panels).



Supplemental Figure S3: In CRWs simulated as a OU process correlation between speed and turning angle vanishes when sampling interval is much larger than the typical persistence time. We simulate the persistent random walk using a model based on OU framework and described by Wu *et al.* [16]. In panel A we assume that every cell have the same persistence time $T_P = P = 0.75$ min and same speed $s = 4.5$ $\mu\text{m}/\text{min}$. We simulated 7200 steps equivalent to 2 hours for 300 cells and sampled for every k^{th} min as shown in the legends (1, 10, 50, 100, 200). In panel B we assume that every cell in the population has different persistence times which was drawn from a lognormal distribution (eqn. (4) with $\mu = 0.2$ and $\sigma = 0.2$), and every cell has a random speed drawn from a lognormal distribution with $\mu = 2$ and $\sigma = 0.2$. We simulated 7200 steps equivalent to 2 hours for 300 cells and sampled for every k^{th} min as shown in the legends. For every set of simulations we also show the average speed (\bar{v}), average turning angle ($\bar{\phi}$) per population, and Spearman rank correlation coefficient (ρ) and p value from the test (that $\rho = 0$).



Supplemental Figure S4: Distribution of estimated persistence times and speeds and simulated speeds for CD8 T cells in the LNs and activated CD8 T cells in the liver. For every trajectory of T cells in LNs (panels A-C) or T cells in the liver (panels D-F) we calculated the persistence time using velocity correlation plots (eqn. (8)) by taking 10 values for the velocity correlations (panels A&D). Trajectories for which less than 5 time points were available we ignored resulting in $n = 1109$ and $n = 251$ trajectories with estimated persistence times for T cells in the LNs and the liver, respectively. For these cells we then also calculated the average speed per cell (panels B&E). To perform simulations of random walks we generated distribution of cell speeds in accord with lognormal distribution (eqn. (4)) with $\mu = 2.8$ and $\sigma = 0.1$ for T cells in LNs (panel C) or $\mu = 2.4$ and $\sigma = 0.2$ for T cells in the liver (panel F). The average persistence time \bar{T}_p and average speed are indicated on individual panels. To plot persistence times on the log-scale, values that are lower than 0.01 were set to 0.01 (in panels A&D).



Supplemental Figure S5: Simulations of CRWs using OU framework do not fully capture the correlation between average turning angle and speed. Simulations were performed as described in **Figure 4A-C** for data for T cells in the LNs and the results were represented using contours of ggplot in R.